Second International Conference on CFD in the Minerals and Process Industries
CSIRO, Melbourne, Australia
6-8 December 1999

CFD MODELING OF NITROGEN DISSOLUTION INTO A STEEL BATH DURING GAS PURGING

Jyrki PITKÄLÄ, Jiliang XIA and Ari JOKILAAKSO

Helsinki University of Technology, P.O.Box 6200, FIN-02015 HUT, Finland

ABSTRACT

In steel production, an important stage is to get composition and temperature distributions homogenous in the ladle before casting. Often this is made with gas purging. For this purpose, the cheapest gas is nitrogen. Disadvantage is that nitrogen dissolves to some extent into liquid steel causing the need for a special nitrogen removal. The present paper focuses on modelling possibilities of the nitrogen dissolution by means of a commercial CFD code. The major interests in the modelling are speed and effectiveness of the dissolution. A user-defined dissolution model has been implemented in the CFX code and the results are compared with industrial measurement data.

NOMENCLATURE

A	surface area of bubble (m^2)
B	body force (buoyancy)
$C_{[N]}$	concentration of nitrogen (wt-%)
C_i	empirical constants in turbulence equations
$c_{\alpha\beta}^{(d)}$	inter-phase drag term
C_D	drag coefficient
f	activity coefficient
F_i	inter-phase forces
G	Gibb's energy (J/mol)
G	production term due to buoyancy (in turb. equations)
k	mass transfer coefficient (m^2/s)
k	turbulent kinetic energy (in turbulence equations)
m	amount of injected nitrogen (kg)
M	mass of melt (kg)
p	pressure (Pa)
P	shear production (in turbulence equations)
Q	gas flow rate (m^3/min)
R	gas constant (8.314 J/K·mol)
r	volume fraction
t	time (s)
T	temperature (K)
U	velocity (m/s)
V	volume (m^3)

Greek symbols

α,β	indicate phases
ε	turbulent dissipation rate
ρ	density (kg/m^3)
μ	dynamic viscosity
σ_i	turbulent Prandtl numbers

Subscripts

ave	average
e	end time
eq	equilibrium
g	gas phase
l	liquid phase
r	reaction
s	initial time

INTRODUCTION

With the gas purging, attempt is made to homogenize the liquid steel for its composition and temperature. The use of the nitrogen instead of argon produces savings, but, on the other hand, causes the growth of the nitrogen content which often leads to the need for removing nitrogen with special methods.

Dissolved nitrogen has a marked effect on the mechanical and the corrosion properties of stainless steels. The nitrogen can be understood as an alloy element or impurity, depending on steel quality and its purpose of use (Rao and Lee, 1985).

Experimental data are needed for developing and validating the mathematical models used in the simulation of gas injection. Extensive studies have been made for the fluid flow and heat transfer in ladles with gas stirred molten metals (Brimacombe et al, 1990, Mazumdar and Guthrie, 1995). However, sparse work has been done for those involved in mass transfer (Battle and Pehlke, 1986).

Most publications assume the mass transfer from the metal into the gas so that the dissolved species in molten metal will move into inert gas, argon. Often would it be, however, cheaper to use nitrogen as blowing gas at a certain stage of the steel process. The nitrogen dissolves in the steel in a large amount. It has been found (in the measurements) that even more than 90% of the nitrogen that is blown into a liquid can be dissolved into the steel (Figure 2 and Table 3). The removal of dissolved nitrogen can cause costs and difficulties which neutralize the advantages of using it as the blowing gas.

It is often very difficult to make direct measurements from an industrial process because of its aggressive conditions. The numerical modelling could facilitate this problem if one could be sure that the mathematical model really describes the situation to be modelled. New stage can be reached by taking small steps with the modelling of the well known phenomena. The modelling of the flow phenomena in gas stirring is already quite well understood and CFD-codes available can moderately simulate gas-liquid interactions.

The present work has been undertaken with the objective of clarifying the mechanism of nitrogen absorption and the ability to model dissolution of nitrogen into steel using the CFX code.

DISSOLUTION PROCESS

Thermodynamics

Nitrogen dissolves into steel in atomic state. In the gas phase, nitrogen appears as diatomic molecule, so the dissolution reaction can be stated as (Steelmaking data sourcebook, 1988):

$$\tfrac{1}{2}N_2(g) = [N] \quad \Delta G = 9.916\frac{\text{kJ}}{\text{mol}} + 20.17\frac{\text{J}}{\text{mol}\cdot\text{K}}T \quad (1)$$

Between the dissolved nitrogen and the nitrogen in the gas phase there is connection that has been derived from the expression of the equilibrium constant:

$$[\text{N}] = \frac{\sqrt{p_{\text{N}_2}}}{f_{[\text{N}]}} e^{-\frac{\Delta G}{RT}} \quad (2)$$

It can be seen that the solubility of the nitrogen into the molten steel is reduced at lower temperature and smaller pressure of the nitrogen. It is also reduced by those alloy elements which increase the activity of the dissolved nitrogen (C and Si) and is enhanced by those alloy elements which lower the activity of the nitrogen (Cr and Mn).

In the normal pressure, the nitrogen tends to dissolve into the molten steel. The nitrogen can be removed by lowering pressure and by flushing gas. At a lower pressure, the purging gas enlarges more strongly, the mixing of the melt can be improved, and the ability of inert gas to dissolve nitrogen can be increased.

Kinetics

There is a general agreement that surface-active elements inhibit both the rate of absorption of nitrogen into molten steel and the rate of nitrogen removal (Rao and Lee, 1985).

Kong et al (1998) have studied the nitrogen desorption from liquid iron. Supposing that dissolving is a reverse phenomenon of desorption, it can be assumed that the dissolution of the nitrogen takes place as follows:

1: Movement of nitrogen molecules from gas phase to boundary layer;

2: Adsorption of nitrogen molecules into the interface;

3: Reaction at the interface;

4: Desorption of nitrogen atoms from interface;

5: Diffusion of nitrogen atoms from gas-liquid interface and moving with liquid flow.

Probably, the interface reaction has the greatest effect on the rate of dissolution, so the rate of the dissolution reaction can be presented with the following equations (Rao and Lee, 1985):

$$\frac{dC_{[N]}}{dt} = \frac{A}{V} k_r \left(C_{[N]_{eq}} - C_{[N]} \right) \quad (3)$$

or

$$\frac{dC_{[N]}}{dt} = \frac{A}{V} k_r \left(C^2_{[N]_{eq}} - C^2_{[N]} \right) \quad (4)$$

At low concentrations of surface active elements (S and O), reaction is first order whereas a second-order behavior prevails at high concentrations of S and O (Rao and Lee, 1985).

MODELLED CASE

The stainless steel is rinsed with inert gas in the ladle. The composition of steel is listed in Table 1 and process parameters in Table 2. Here, an attempt has been made to choose a typical sample of the nitriding tests done. Figure 1 shows a schematic view of the ladle to be considered in the present study. The diameter of the vessel is 2.4 metres and its height is 3.0 metres. The porous plug with which the gas is injected is asymmetrically placed to the bottom of the vessel.

C: 0.033	Si: 0.5	Mn: 1.48	P: 0.025
S: 0.001	Cr: 17.9	Ni: 8.56	Mo: 0.18
Ti: 0.003	$N_{2,s}$: 0.0325	$N_{2,e}$: 0.0385	

Table 1: Composition of steel (mass-%).

M (kg)	T (K)	Q (m^3/min)	t(s)	V_{N_2} (m^3)	m_{N_2} (kg)
90'000	1800	0.371	900	5.6	6.8

Table 2: Process parameters.

Within these conditions and composition, the equilibrium content of the nitrogen in steel, $C_{[N]_{eq}}$, is about 0.11 % (1100 ppm). In practice this value is rarely reached. For example, the nitrogen content varies after the pouring in AOD process between 200 and 900 ppm (Kishida et al. 1993).

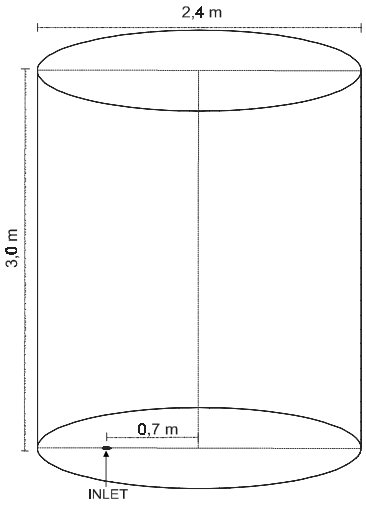

Figure 1: Schematic diagram of geometry.

MATHEMATICAL MODEL

In this work a commercial CFD-code CFX has been used to solve the conservation equations. The Eulerian two-fluid approach is used. The modelling of the momentum transfer in isothermal case has been described by Vaarno et al. (1998). Generally, in this kind of multi-fluid model, there is separately one solution field for each phase. Transported quantities interact via inter-phase terms. The pressure in both phases is assumed to be the same within a computational cell. Field equations for each phase are weighted with the volume fraction of that phase. The model is solved using the Inter-Phase Slip Algorithm (IPSA). The equations to be solved in isothermal case are continuity and momentum equations for both (liquid and gas) phases (AEA, 1997):

$$\frac{\partial}{\partial t}\left(r_\alpha \rho_\alpha\right) + \nabla \cdot \left(r_\alpha \rho_\alpha U_\alpha\right) = 0 \tag{5}$$

$$\begin{aligned}\frac{\partial}{\partial t}\left(r_\alpha \rho_\alpha U_\alpha\right) + \nabla \cdot \left\{r_\alpha\left[\rho_\alpha U_\alpha \otimes U_\alpha - \mu_\alpha\left(\nabla U_\alpha + \left(\nabla U_\alpha\right)^T\right)\right]\right\} \\ = r_\alpha\left(B - \nabla p_\alpha\right) + \sum_{\beta=1}^{N_P} c_{\alpha\beta}^{(d)}\left(U_\beta - U_\alpha\right) + F_\alpha\end{aligned} \tag{6}$$

The drag force is taken into account for the interphase interactions. The turbulence equations have been solved for both phases. The dissolving effect has been taken into account as source terms in the governing equations.

Turbulence

Nowadays, the CFD codes contain several different turbulence models. In the present study, the standard k-ε model (Launder and Spalding, 1974) was chosen. It requires solving two dimensional transport equations, one for turbulent kinetic energy:

$$\frac{\partial \rho k}{\partial t} + \nabla \cdot \left(\rho U k\right) - \nabla \cdot \left(\left(\mu + \frac{\mu_T}{\sigma_k}\right)\nabla k\right) = P + G - \rho\varepsilon \tag{7}$$

and the other for dissipation rate of turbulent energy:

$$\begin{aligned}\frac{\partial \rho \varepsilon}{\partial t} + \nabla \cdot \left(\rho U \varepsilon\right) - \nabla \cdot \left(\left(\mu + \frac{\mu_T}{\sigma_S}\right)\nabla \varepsilon\right) = \\ C_1 \frac{\varepsilon}{k}\left(P + C_3 \max(G,0)\right) - C_2 \rho \frac{\varepsilon^2}{k}\end{aligned} \tag{8}$$

Here the model constants are those proposed by Launder and Spalding (1974). The bubbles increase the turbulence of the continuous phase but this phenomenon has not been included in the calculation because according to Vaarno (1998) there is no generally accepted mathematical formulation for bubble-induced turbulence.

Drag force between the phases

The momentum transfer between the phases takes place on the basis of the drag function, which can be calculated as follows (Davidson, 1990):

$$F_l = -F_g = \frac{3C_D}{4d_b} r_g \rho_l \left|\vec{u}_g - \vec{u}_l\right|\left(\vec{u}_g - \vec{u}_l\right) \tag{9}$$

The drag coefficient C_D depends on the (local) flow regime and the liquid properties. There are several different functions for the calculation of the drag coefficient, C_D. In this study, the code has been allowed to calculate the drag coefficient automatically according to its own definitions.

Bubble size

In the calculations, the bubbles are assumed to have an average diameter of 6.0 mm. It is assumed to characterize the whole bubble size distribution. Kitamura et al (1996) have supposed 10 - 50 mm to be an argon bubble size, and size of CO bubble 5 - 10 mm in this kind of situation. According to Mazumdar and Guthrie (1995) porous plug produces more, uniformly distributed, smaller size bubbles. The constant bubble size is one of the most serious restrictions in the model. The bubble size affects inter-phase forces and mass transfer area, so the characteristic value should be defined accurately. In the calculations which are demonstrated in this paper the dissolution of nitrogen does not affect a bubble size but only to the number of the gas bubbles in the calculation cell. In the future it is of importance to take into account the change of the bubble size during dissolution reaction.

Boundary conditions

The calculation domain has been divided into 18750 cells (25 x 25 x 30) and the calculations have been carried out in three dimensions. The free surface is assumed to be a flat and frictionless wall, through which the undissolved gas phase is allowed to escape. Nitrogen gas enters the domain as a mass source and is removed using a sink term. In CFX the user has to take care of this by using his/her own subroutines. The sink term has been set based on the vertical velocity of the bubbles at the active cells next to the degassing boundary.

Due to the character of the dissolving reaction the transient calculations must be performed. At the initial stage the average time step is about one millisecond

(0.001 s). After this the time step can be lengthened even to a value 0.1 seconds.

The dissolving tendency of the injected nitrogen is here presented with an equation (4). Second order reaction was chosen here. According to Rao and Lee (1985), and Kong et al. (1998), this is the reasonable choice. Numerical values for equation (4) used in calculations are $C_{[N]eq}$ = 0.0011, k = 0.2.

RESULTS AND DISCUSSION

The results which are demonstrated here are preliminary results that have been obtained from the development of the mass transfer model. An attempt has not been made to model the whole process at this stage at all. On the basis of the results the functionality of the model has been estimated.

Figure 2 shows the results obtained from industrial measurements (Hooli, 1998). In these measurements, the nitrogen content of steel has been determined before and after blowing. The gas flow rate and handling time have been changed between the blowings. Table 3 shows the gas flow rates and blowing times used in measurements and total amounts of injected nitrogen. The results of the measurements indicate the ability of steel to dissolve nitrogen. It can be seen from these results that the dissolution is mainly dependent on the amount of gas and depends not much on the gas flow rate or blowing time.

Case No.	t (s)	Q m^3/min	N_2 kg	$\Delta C_{[N]}$ meas.	$\Delta C_{[N]}$ theor.	Dissolved
1	600	0.571	6.96	0.0065	0.0077	84 %
2	900	0.371	6.79	0.0060	0.0071	84 %
3	900	0.713	13.05	0.0140	0.0150	93 %
4	540	0.856	9.39	0.0095	0.0100	95 %

Table 3: Measurements (Hooli, 1998).

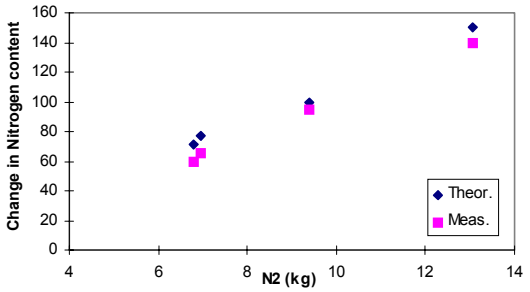

Figure 2: Change in the nitrogen content as a function of the amount of the nitrogen injected into steel (measured, Hooli, 1998).

In this work the modelled case was number 2. Blowing time was 15 minutes (900 s) and gas injection rate 0.371 m^3/min, which means the mass flow rate of $7.54 \cdot 10^{-3}$ kg/s. Thus the total amount of nitrogen injected into steel was 6.79 kg. Nitrogen content is shown in the Figure 3 as a function of time calculated by the CFX code using the above proposed dissolution model. It is seen that the average content of the dissolved nitrogen increases with the time during this period. However, the theoretical average increase calculated from the measurement data is lower. A better agreement is probably obtained by modifying the coefficients of the model. The comparison with measured data can also be seen in the Figure 4, where change on the nitrogen content of steel is plotted as a function of total mass of injected nitrogen.

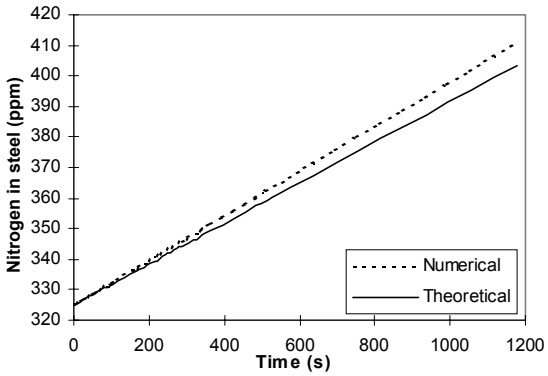

Figure 3: Change of the average nitrogen content.

With the gas flow rate used in the experiments, the average change in the nitrogen content was $6.67 \cdot 10^{-6}$ %s^{-1}. $C_{[N]ave}$ changed from 0.0325 % to 0.0385 % within 15 minutes. At the beginning, in our simulations this rate of change is $1.4 \cdot 10^{-5}$ %s^{-1}, but is rapidly decreasing within time reaching finally value $7.2 \cdot 10^{-6}$ %s^{-1}. This decreasing of the dissolution rate is understandable because the difference to the equilibrium content is reduced all the time and the driving force of the dissolving reaction becomes smaller.

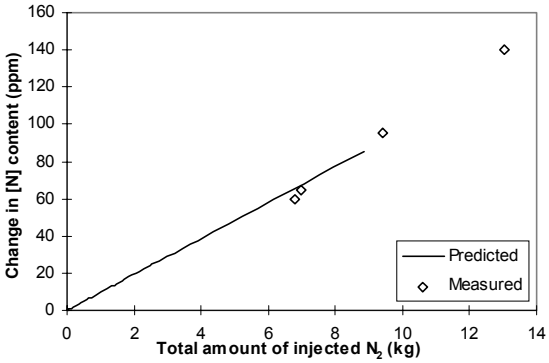

Figure 4: Simulated and measured N_2 contents.

It is to be noted that this is only a preliminary model on the way towards the tool with which it is possible to describe and study the dissolving process better. A few significant restrictions are still connected to the model. First of all, attention is only paid to the dissolution from the blowing gas to the liquid metal. However, the dissolving reaction is reversible, to which the model does not pay attention at the moment. Further, in an actual reactor many kinds of interactions happen between liquid and slag, which have not yet been considered.

The momentum transfer between the phases is reduced if the dissolution reaction is taken into account. Remarkable amount of injected gas is dissolved. Figure 5 shows the velocity vectors at the nozzle plane when dissolution is not taken into account. Figure 6 shows this situation with

same gas flow rate with dissolution model. It can be seen that velocities are smaller than in the case, where the whole gas is inert.

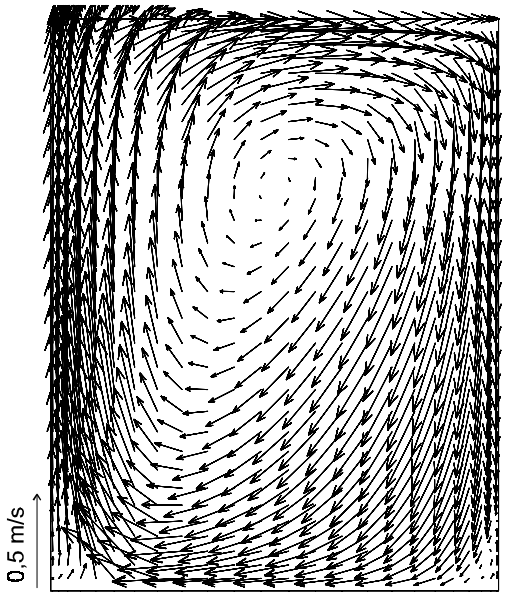

Figure 5: Flow velocity vectors at nozzle plane (calculated without dissolution model).

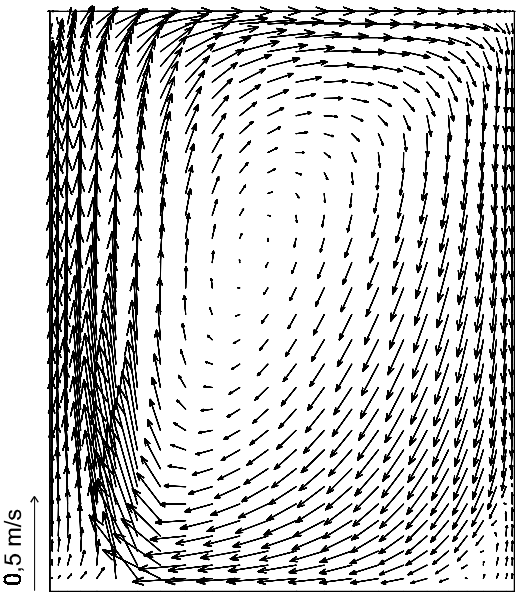

Figure 6: Flow velocity vectors at nozzle plane (calculated with dissolution model).

CONCLUSIONS

In this paper, some preliminary results of the modelling of the dissolution reaction of the nitrogen into liquid steel are described. The main purpose has been to study the suitability of a CFD code for the modelling of this kind of phenomenon. A simplified model for the dissolution reaction has been implemented and it was found that the fluid flow phenomena in steelmaking ladle coupled with dissolution of injected nitrogen gas into the liquid steel can be predicted using the CFX code. The first results suggests that the nitrogen dissolution tendency is in a fair agreement with the measured data. Naturally, a lot of further work and validation is needed. Nitrogen dissolution effect on the liquid flow was well predicted, but this was not, however, possible to verify due to lack of measured velocity data of a real ladle.

ACKNOWLEDGEMENTS

The authors wish to thank the National Technology Agency of Finland (Tekes), and the national CFD Technology Programme for financing and Outokumpu Polarit Oy for permission to publish this paper.

REFERENCES

AEA Technology (1997), *CFX-4.2 Solver Manual*. CFX International, Oxfordshire, UK, December 1997.

BATTLE, T.P. and PEHLKE, R.D. (1986), "Kinetics of nitrogen absorption/desorption by liquid iron and iron alloys", *Ironmaking and Steelmaking,* **13,** 176-189.

BRIMACOMBE et al. (1990), "Process dynamics: Gas-Liquid". *Proceedings of the Elliot Symposium on Chemical Process Metallurgy.* Cambridge (MA), June 10-13 1990. Warrendale, PA, USA, 343-412.

DAVIDSON, M. R. (1990), "Numerical calculations of two-phase flow in a liquid bath with bottom gas injection. The central plume.", *Applied Mathematical Modelling*, **14**, 67-76.

HOOLI, P. and KURONEN, T., Private communication, Outokumpu Polarit, Tornio, Finland, Dec. 1998.

KISHIDA, T et al. (1993), "Development of New Stainless Steelmaking Processes", *Scand. J. Metallurgy,* **22**, 173-180.

KITAMURA, T. et al. (1996), "Mathematical model for Nitrogen Desorption and Decarburization Reaction in Vacuum Degasser", *ISIJ International,* **36**, 395-401.

KONG, S-J. and LEE, H-G. (1998), "A new interpretation of mechanisms of nitrogen desorption from liquid iron", *Steel Research,* **69,** (3) 85-91.

LAUNDER, B. E. and SPALDING, D. B. (1974), "Numerical Computation of Turbulent Flows" *Computer Methods in Applied Mechanics and Engineering,* **3**, 269-289.

MAZUMDAR, D. & GUTHRIE, R. I. L. (1995), "The physical and mathematical modelling of gas stirred ladle systems", *ISIJ Int*, **35**, 1-20.

RAO, Y. K and LEE, H. G., (1985), "Rate of nitrogen absorption in molten iron: Part 1 experimental", *Ironmaking and Steelmaking,* **12**, 209-220.

Steelmaking data sourcebook (1988) The Japan Society for the Promotion of Science. The 19th Committee on Steelmaking, Rev. ed. New York (NY): Gordon and Breach Science, 325 p.

VAARNO, J. et al. (1998), "Modelling gas injection of a Peirce-Smith-converter", *Applied Mathematical Modelling,* **22,** 907-920.